IEEE Open Access Journal of
Power and Energy

Received 12 November 2022; revised 2 February 2023; accepted 10 February 2023.
Date of publication 15 February 2023; date of current version 24 February 2023.

Digital Object Identifier 10.1109/OAJPE.2023.3245993

Coordinated Planning of Electric Vehicle Charging Infrastructure and Renewables in Power Grids

BO WANG [1] (Member, IEEE), PAYMAN DEHGHANIAN [2] (Senior Member, IEEE), AND DONGBO ZHAO [3] (Senior Member, IEEE)

[1]Amazon Web Services, Seattle, WA 98108 USA
[2]Department of Electrical and Computer Engineering, George Washington University, Washington, DC 20052 USA
[3]Eaton, Golden, CO 80401 USA

CORRESPONDING AUTHOR: B. WANG (wangbo@gwu.edu)

ABSTRACT This paper proposes a new planning model to coordinate the expansion of electric vehicle charging infrastructure (EVCI) and renewables in power grids. Firstly, individual electric vehicle (EV) charging behaviours are modeled considering EV customers adopting smart charging services as the main charging method and those using fast charging, super fast charging and battery swapping services as a complementary charging approach. Next, EV aggregation and the associated system economic dispatch model are built. A novel model predictive control (MPC) learning approach is then proposed to iteratively learn the correlation between different types of EV charging loads and the EV interactions with renewables and other generating units in modern power grids of the future. The simulation results demonstrate that the proposed approach can be used to quantify the ratio of different types of charging loads in a region and strategically guide on the integration of EVs and renewables to achieve the clean energy transition goals. The proposed framework can also be used to decide charging capacity needs in a charging demand zone.

INDEX TERMS Electric vehicle charging infrastructure (EVCI), model predictive control (MPC), power system planning, predictive learning, queuing model.

NOMENCLATURE

A. Indices

i	Index for generating units (1,...,n).
k	Index for time steps (1,...,K).
m	Index for iterations.

B. Parameters

α	The queuing probability for EVs in a charging station.
α_c, α_d	Charge/discharge efficiency of the battery.
Δt	Length of the time step.
γ	Penalty factor for deviations from PEV daily energy consumption.
Λ_R	Total renewable power generation.
ρ	Ratio of reserve to EV smart charging demand.
ς	The maximum flexibility of PEV loads.
c_d	Degradation cost of battery per MWh.
D	Constant battery swapping time in BSSs.
E_C	PEV forecasted energy demand in the next 24 hours.
E_s	Total EV energy consumption using battery swapping services.
J_{lb}	The lower bound for 7-day economic dispatch.
L_F	Electricity demand for EVs that only use fast charging service.
L_O	Original electrical load.
V_C	Curtailment cost of renewables.

C. Variables

$\Delta P_{G,i}$	Ramp rate of generating unit i.
λ	Average arrival rate of EVs in the peak hour.
μ	Average service rate of EVs in the peak hour.
B_s	Energy stored in a battery swapping station.
c	The capacity of a charging station i.
$C_i(P_{G,i})$	Operating cost function of generating unit i.
J_m	The 7-day economic dispatch outcome in iteration m.
L	The average number of EVs in the system during the peak hour.

L_c Total energy allocated to PEVs.
L_q The average number of EVs in the queue during the peak hour.
L_s The average number of EVs in service during the peak hour.
P_C Renewable power curtailment.
P_G Active power of generating units.
P_{net} Vector of the net generation.
P_R Effective renewable power integrated into the system.
u_c Supplied power from the power grid to BSS.
u_d Delivered power from BSS to the power grid.
u_l PEV charging demand.

I. INTRODUCTION

TRANSFORMATION of the energy sector has been initiated in several countries to achieve the net-zero emission goals by 2050 [1]. Electrification of vehicles emerges as a crucial economy-wide strategy to reduce greenhouse emissions. There are several electric vehicle (EV) models currently available in the market. Different types of EV supply equipment [2] and EV charging stations [3] are proposed to address the charging needs and mitigate the challenges of widespread EV integration in power grids. Advanced metering infrastructure [4] and distributed energy resource (DER) communication network are also being growingly built to integrate large-scale EV loads using direct load control [5]. Larger penetration of EVs is currently hindered by inadequate charging infrastructure [6]. Incentives are provided by federal and state governments to promote the deployment of EV charging network. EV charging infrastructure (EVCI) planning has also become a research hot-spot in the literature.

The EVCI planning based on individual EV charging facilities has been studied in the literature. The charging demand of a fast charging station (FCS) located near a highway exit is estimated in [7]. Ratio assessment of EV charging facilities based on charging costs of EVs in a single smart charging station (SCS), battery swapping station (BSS), or with an uncoordinated home charger are discussed in [8]. The EV charging demand and EV routing to the existing charging facilities in a local demand zone are also explored when the EV charging facilities are not sufficient [9], [10]. The above research only considers retail markets under low levels of EV penetration. However, EVCI are shaped at regional levels, and due to the high investment costs and long-term operation and maintenance requirements, system-level planning of charging facilities is in high demand globally.

The expansion of FCSs in a region is studied in [11] and [12] assuming that the EV charging demand is proportional to the traffic flow. Nationwide FCS planning is proposed in [13] for EVs with long-distance trips. Accommodation of such widespread installation of FCSs, however, calls for a significant upgrade in power networks demanding considerable costs and resources [14]. Also, most EV charging currently occurs at homes when home charging is feasible [15]. The cost-effective siting of EVCI in a metropolitan area is investigated in [16] considering uncoordinated operation of home charging and FCS. However, uncontrolled charging of EVs might jeopardize the operation of the power grid [17]. Smart charging (SC) can be used in the SCSs to coordinate either the home charging in a community or public charging in a charging station. The operation and capacity of aggregated BSSs are discussed in [18] to maximize the BSSs aggregation profit considering their potential in becoming a part of the EVCI mix. Nevertheless, these planning models were not able to coordinate different types of charging facilities including SCSs, FCSs, super fast charging stations (SFCSs) and BSSs at the regional level, and joint expansion planning of EVCI and renewables has not been explored. To fill in this gap, a master plan is needed to coordinate the planning of all different types of charging facilities and to quantitatively guide on EVCI expansion. The plan should not only optimize specific charging facility expansion, but also consider the usage of increasing flexible EV load to adapt to the increasing intermittence in the renewable power outputs such as wind and solar [19].

The majority of the recent literature on the topic, however, either focuses on the deployment of FCS in urban areas, or apply simplified demand-side models for system-level planning without investigating SC strategies [20]. The planning and competition among service providers for commercial charging stations are studied in [21] considering the power distribution system and transportation network, in which SC is not included. Considering the significant impact of high EV penetrations on the market electricity prices, the cost production model is used to simultaneously deploy charging infrastructure and expand the capacity of clean energy generators in [22], but the studied topic is limited to planning for the FCS. Different types of charging technologies are studied in [23], where SCS and BSS planning are not considered, and the EVCI planning under renewable integration only tries to mitigate the system peak load.

This paper extends our previous work [24] and [25] and aims at comprehensively addressing the knowledge gap on the coordinated planning of both EVCI and renewables. Compared to this paper, [24] investigates EV charging management algorithm, and [25] identifies the parameters and flexibility range of the aggregated EV load models in the daily operation of power grids, in which EVCI planning is listed as a future work. Besides, a new EV customer behavior model is here built, where we assume SC is the main charging method, and fast charging (FC), super-fast charging (SFC) and battery swapping (BS) are complementary charging methods. Note that BS is used in the previous papers as the only complementary charging method. Furthermore, the unknown interdependence among different EV charging loads is identified iteratively using a proposed predictive learning model. Thus, system identification of future smart grids with EV loads and renewables is achieved. In previous work [25], only the aggregated EV load and its flexibility range for the daily operation are identified, which is limited to the parameter

identification of a predefined model. The main contributions of this paper are:

1) Quantify the nearly-optimal EV charging load ratio in different regions under different EV and renewable penetrations, when SC is the main charging method and FC, SFC and BS alternatives are the complementary charging methods.
2) Identify the interdependence among different EV charging loads and interactions of EVs and renewables in smart grids using the proposed predictive learning method. Instead of using given EV load profiles [23] for EVCI planning, individual EV activities and the system cost production model are incorporated in the model to optimize the EV charging load ratio, and at the same time, achieve a system identification.
3) Estimate the capacity of different EV charging stations including SCS, FCS, SFCS and BSS, to support potential large-scale EV charging demand and high renewable penetration in power grids, and coordinate EVCI expansion planning among different stakeholders cost-effectively.

The rest of this paper is organized as follows. Section II presents the mathematical formulation of the proposed model and the predictive learning method to assess the EV charging loads and characterize the EV interactions with renewables. Section III introduces the capacity provisioning of different EV charging stations. Section IV presents the case studies. Section V discusses applications of the proposed models in practice, followed by the conclusions in Section VI.

II. SYSTEM IDENTIFICATION OF POWER GRIDS WITH MASSIVE INTEGRATION OF EVs AND DERs

This section first introduces the individual EV customer behavior model. Then the aggregation of different types of EV loads and the integration into a system-level economic dispatch model are proposed. The system identification is achieved by using the proposed predictive learning model.

A. LOWER-LEVEL EV ACTIVITY SIMULATION

The EV customers that only use FC and SFC services are typically found to charge their EVs mainly during the daytime, featured with a routine charging behavior [26]. Hence, load forecasting algorithms can be used directly to forecast the aggregated load featured as an inelastic demand. The aggregated BS load by EV customers that only use BS services can also be regarded as inelastic load. Accordingly, only the aggregated EV loads are here simulated for these types of customers.

To capture all charging scenarios of EVs that mainly use SC, the model incorporates FC, SFC and BS as complementary charging methods for these customers when the SC could not satisfy their energy demands during trips. Note that SC in this paper refers to all the level-2 home charging, public parking charging, and workplace charging. Figure 1 illustrates the key decisions for these types of customers. When the EV is parked and need to be charged, if it subscribes the BS service as a complementary charging method, the EV will use SC at SCSs. The energy demand of SC is 1.2 times larger than the minimum requirement set by the customer, and need to be met upon EV departure, but limited to its charging as well as EV battery capacities. When the SC could not satisfy the charging demand, the EV customer will swap the depleted battery with a fresh one in the BSS during the trip. If the EV does not subscribe the BS service as a complementary charging method, the EV customer will check whether the SC could satisfy the trip energy demand. FC or SFC will be used based on the EV charging demand as long as SC could not provide enough mileage for their next trip. FCS and SFCS will start to charge EVs upon their arrival. Although the BS service is not subscribed by these EV customers, they can still swap the depleted batteries during the trip when their charging demand could not even be met by SFC. Note that human-in-the-loop decision and system interactions with other energy resources exist. Hence, the individual EV activity is simulated for this type of customer.

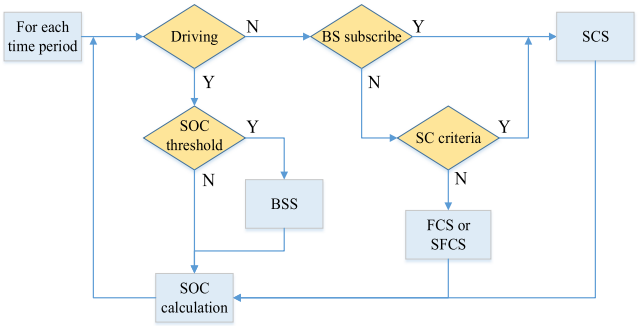

FIGURE 1. **The flowchart of EV states for smart charging EV customers with FC, SFC and BS as complementary charging methods.**

B. HIGHER-LEVEL SYSTEM ECONOMIC DISPATCH

The system-level look-ahead economic dispatch model considers different types of EV charging load. The objective function (1) minimizes the total operational cost by dispatching both generator power and EV loads.

$$\min J = J_1 + \sum_{k=1}^{K} (J_2 + J_3 + J_4) \tag{1a}$$

$$J_1 = \gamma (L_c(K+1) - E_C)^2 \tag{1b}$$

$$J_2 = V_C P_C(k) \tag{1c}$$

$$J_3 = \sum_{i=1}^{n} C_i(P_{G,i}(k)) \tag{1d}$$

$$J_4 = 2c_d u_d(k) \tag{1e}$$

The penalty cost in (1b) accounts for plug-in EV (PEV)'s daily energy demand deviation, i.e., aggregated SC EV load

plus its complementary FC and SFC loads. The cost of curtailed renewable energy is shown (1c). The quadratic operational cost of fuel-based generators is in (1d). Equation (1e) represents the degradation cost of batteries in BSSs under the vehicle to grid (V2G) operating mode when EV batteries are discharged causing extra battery cycles, and hence, the cost is double. The system constraints for the economic dispatch model are presented in (2)-(15) as below.

$$\sum_{i=1}^{n}(P_{R,i}(k)+P_{G,i}(k))+u_d(k)-u_c(k)-u_l(k) = L_O(k)+L_F(k) \quad \forall k \tag{2}$$

$$P_{G,i}(k+1) = P_{G,i}(k)+\Delta P_{G,i}(k) \quad \forall k\ \forall i \tag{3}$$

$$P_{G,i}^{min} \le P_{G,i}(k) \le P_{G,i}^{max} \quad \forall k\ \forall i \tag{4}$$

$$\Delta P_{G,i}^{min} \le \Delta P_{G,i}(k) \le \Delta P_{G,i}^{max} \quad \forall k\ \forall i \tag{5}$$

$$P_{C,i}(k)+P_{R,i}(k) = \Lambda_{R,i}(k) \quad \forall k\ \forall i \tag{6}$$

$$0 \le P_{R,i}(k) \le \Lambda_{R,i}(k) \quad \forall k\ \forall i \tag{7}$$

$$\boldsymbol{H}\cdot\boldsymbol{P_{net}}(k) \le \boldsymbol{F} \quad \forall k \tag{8}$$

$$L_c(k+1) = L_c(k)+\alpha_c u_l(k)\,\Delta t \quad \forall k \tag{9}$$

$$0 \le L_c(k) \le (1+\varsigma)E_C \quad \forall k \tag{10}$$

$$u_l^{min}(k) \le u_l(k) \le u_l^{max}(k) \quad \forall k \tag{11}$$

$$B_s(k+1) = B_s(k)+(\alpha_c u_c(k)-(\alpha_d)^{-1}u_d(k))\Delta t - E_s(k) \quad \forall k \tag{12}$$

$$B_s^{min} \le B_s(k) \le B_s^{max} \quad \forall k \tag{13}$$

$$0 \le u_c(k) \le u_c^{max} \quad \forall k \tag{14}$$

$$0 \le u_d(k) \le u_d^{max} \quad \forall k \tag{15}$$

Equation (2) enforces the power balance constraint, where aggregated EV load for customers only using FC and SFC is represented by L_F. The state equations of fuel-based generators are given by (3)–(5). The output of the ith generator at the next time step in (3) is equal to the generator's current power plus its ramp. The physical capacity constraints for each generator is given by (4). Ramp limits for generators in next several time intervals are shown in (5). The variable renewable power is expressed by (6). The effective renewable power generation integrated into the grid plus the curtailment is equal to the total renewable power generation. The amount of the renewable power generation integrated into the grid depends on the total renewable power generation as described in (7). Equation (8) represents the transmission line power flow limits. H is the power transfer distribution factor (PTDF) matrix. The vector storing intermediate calculation of the net generation at all buses is given by $\boldsymbol{P_{net}}$. The vector of the transmission line limits is $\boldsymbol{F}$.

Equations (9)-(11) express the state and control constraints of PEV loads. The total load is modeled as virtual batteries, where the battery energy increases gradually, and the charging limits vary with time. L_c is the cumulative energy that is expected to be allocated; equation (9) presents that the $L_c(k+1)$ at the next time step is equal to $L_c(k)$ plus the actual charging power u_l allocated to EVs at time step k. The EV demand is restricted by (10), and its maximum flexibility is reflected by ς. u_l is constrained to its lower and upper bound limits in (11). The aggregated PEV model is from [24] and [25]. It is based on the centralized charging method for EVs using direct load control in which the availability of PEV customers and charging requirements of individual PEVs are fully considered. Bidirectional signals communication are enabled between EVs and the power grid. Three information including EV departure time, minimum state of charge (SOC) requirement, and the current SOC are collected from individual EVs to calculate the time-dependent aggregated charging constraints $u_l^{min}(k)$ and $u_l^{max}(k)$, once the customers (in Fig. 1) plug in their vehicles. The aggregated charging power u_l in each time step is calculated by the economic dispatch model and distributed proportionally to each charging station. Charging stations will then allocate the power to EVs by using a sorting based algorithm, which prioritizes EV charging demands considering their departure time and charging demand.

The state and control constraints of the aggregated BS load [25] is determined by equations (12)-(15), where V2G functionality is considered in the BSS. The energy stored in the BSS at the next time step in (12) is equal to the current BSS energy plus the charged energy, minus the discharged energy and BS load. The BS load E_s is formulated as an additive disturbance to the BSS and includes both the BS demand by the customers only using BS service and the complementary BS demand from EVs in Fig. 1. While the BSSs have different battery swapping load at each time step, they have fixed battery capacity. The battery storage capacity of the BSS (B_s) in (13) and the charging and discharging power (u_c and u_d) in (14) and (15) are limited to the corresponding thresholds. Note that the battery degradation cost for additional V2G cycles and charging efficiency are modeled in the optimization problem, where BSS will not charge and discharge at the same time.

It is worth mentioning that individual EV behavior, including EV availability and trips, are imported to the optimization model to decide on both the state of EV based on the flowchart presented in Fig. 1 and the SOC of each EV. So, the decision to use either SC, FC, SFC or BS services and calculation of EV SOC is done by individual EVs in the lower-level model. From customer point of view, decision to use different charging services is made by themselves based on their travel demands and preferences, and they only need to set the estimated depart time and expected SOC of EVs when they use SC service. From the perspective of the system operator, only the aggregated charging constraints and charging power are changed for PEVs, and only additive BS load is changed for BSSs. The higher-level mathematical model for the PEVs remains the same as in our previous work [25]. Note that the system operator should provide a lower electricity price for SC EVs since the aggregated SC EV loads provide additional flexibility to the grid. The rate design and incentives for these SC EVs are out of the scope of this paper.

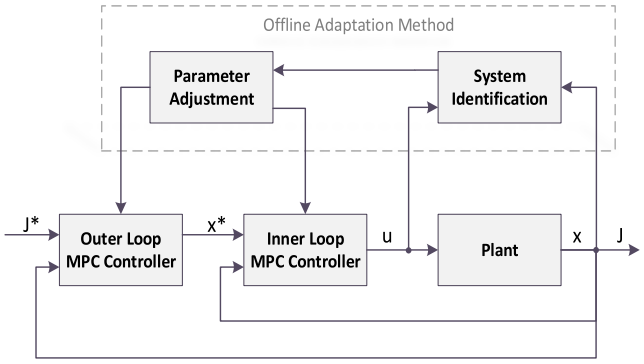

FIGURE 2. The proposed predictive learning model: MPC learning.

C. INTERACTION OF EVs WITH DERs IN THE POWER GRID

In order to have a promising expansion planning decision of EVCI, one needs to estimate the correlation between different charging mechanisms and the interaction of DERs and EVs in the smart power grids of the future. Predictive learning is the framework used for the estimation of predictive data-analytic models, which employ historical data and analytical techniques to predict the future outcomes [27]. A novel predictive learning model, model predictive control (MPC) learning, is proposed in this paper to predict the future EV charging loads. Different from predictive learning via machine learning for systems where neural networks are used as a black box model [28], MPC learning employs double closed-loop MPC [24] and adaptive control [29]. Thus, it relies on explicit models and can provide performance guarantees. The proposed framework for the MPC learning model is illustrated in Fig. 2.

1) DOUBLE CLOSED-LOOP MPC

The double closed-loop MPC model in [24], which is the part excluding offline adaptation method circled by dashed line in Fig. 2, is firstly used to optimize the system costs without violating the individual EV customer charging constraints. It identifies charging load correlations for EV customers in Fig. 1, considering system dynamics. Specifically, the outer loop runs a 24-hour-ahead economic dispatch in equations (1)-(15) with the time step of 1 hour, and passes the 3-hour-ahead dispatch targets of virtual batteries to the inner loop. The inner loop tries to follow the dispatch targets sent from the outer loop by calculating the value of system control variables using the economic dispatch model. It then coordinates individual EV charging through two-way communications with the system operator. The time step of the inner loop is 5 minutes. The plant is the power grids with large-scale integration of EVs and DERs. The double closed-loop MPC will quantify the SC load and its correlation with other charging loads under given prediction values. Considering the disturbance, both loops will adjust the control policies based on the measured state variables during the next step. Certainty equivalence MPC is used in both loops for planning purposes, and uncertainties in renewables and EV loads are fully considered in the economic dispatch model.

2) OFFLINE ADAPTATION AND ITERATION

The offline adaptation method, represented in dashed lines in Fig. 2, will update the system parameters in the economic dispatch model once the charging loads are identified. The system will then iterate until the total cost reaches a low-enough optimality gap. Specifically, once the online computation is terminated, the results are used to update the parameters of the virtual batteries in equations (9)-(11) and equations (12)-(15). The economic dispatch model with updated parameters will then be used in the double closed-loop MPC model for system identification again in order to achieve a better parameter estimation during each iteration. The iterations will be terminated once a certain desired level of accuracy is reached. The stop criteria for iteration m ($m \geq 2$) are expressed as

$$\frac{J_m - J_{lb}}{J_{lb}} \leq TH \tag{16a}$$

$$J_m \geq J_{m-1} \quad or \quad \frac{J_m - J_{m-1}}{J_{m-1}} \leq \epsilon \tag{16b}$$

where the parameter TH is fixed to 10%, so the difference between the economic dispatch cost J_m and its lower bound J_{lb} should be less than 10%. The lower bound value is derived using hourly data with the assumption of fully-controllable smart charging load and perfect knowledge on the other loads. The parameter ϵ is fixed to 0.1%, so the iterations will stop once the total cost of the system in the current iteration is higher than that in the previous iteration, or the costs are sufficiently close to each other.

The implementation steps of the MPC learning method is shown in Fig. 3, which deploys an indirect adaptive control scheme [30]. The MPC learning method firstly estimates the aggregated EV loads for different EV charging methods using the double closed-loop MPC algorithm. The estimates for these parameters are then updated during offline adaptation to calculate the system dispatch results and the EV load control strategies until the results meet the stop criteria in (16). With iterations, the overall MPC learning model is able to estimate the unknown dependency among different EV charging methods by reducing the prediction error gradually. Hence, the MPC learning method can provide a nearly optimal solution to the system operation under the situation that the future SC and its inter-dependency with other charging methods are less understood, and at the same time, identify the charging loads for a smart grid with high EV and renewable penetrations. The temporal EV load simulation results can be used to calculate the ratio of EVs in the services available at different types of charging stations in order to obtain a promising EVCI expansion planning strategy.

It is worth noting that the proposed MPC learning method allows for accurate representation of individual EV charging constraints during each iteration. It is different from machine learning methods which learn customer charging and driving

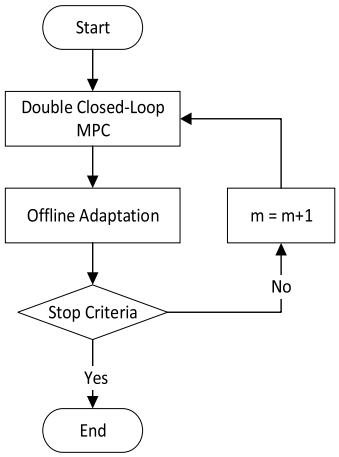

FIGURE 3. Flowchart describing the implementation steps of the MPC learning method.

decisions [31] and face difficulties at incorporating complex EV physical constraints [32]. Besides, MPC learning applies the adaptive control to high-level objectives to identify a smart grid of the future with some unknown parameters, while most existing adaptive control methods are limited to lower-level control applications such as the one in [33].

III. EVCI EXPANSION PLANNING

The clean energy transition objectives and the electric utility planning are the main driving factors for the growing DER penetrations. The projection of EV penetration level can also be made by electric utilities to reduce the greenhouse gas emissions. Once the system-level DER and EV penetration targets are set, the MPC learning model can simulate interaction among EVs with DERs in the grid and identify the temporal EV loads. The system planners can also adjust the EVCI and DER expansion targets based on the simulation results. If the spatial information of EVs can be acquired or sampled, the simulation model can return the spatial-temporal results of the EV charging loads as individual EV trips are simulated. However, such detailed information is hard to obtain in practice, and available data is limited, especially at the regional level with a large number of integrated EVs [34]. Future work needs to address these research gaps. In this paper, we study a region with customers that mainly use smart charging and use other charging methods as complementary methods. The number of charging facilities needed in a local charging demand zone is estimated in this Section.

A. CAPACITY PROVISIONING OF SCSs

The SC usually requires chargers to turn on/off EVs to optimize the economic dispatch cost, and EVs are parked in the parking lots for several hours. Therefore, extra chargers should be installed to enable an opportunity to reserve a certain level of capacity ρ to meet the peak demand and capture the stochastic EV customer behavior. If the average number of EVs that are being served in the peak hour is L_s, the capacity of the SCS is then assessed via the following equation:

$$c = \frac{L_s}{(1-\rho)} \tag{17}$$

B. CAPACITY PROVISIONING OF FCSs AND SFCSs

The EVs at FCSs and SFCSs are normally charged upon arrival. The arrivals of EVs at FCS and SFCS during a specific period are typically featured with a Poisson distribution with rate λ. Each charger has an independently and identically distributed exponential service-time distribution with mean T $(1/\mu)$. It is assumed to have sufficient charging facilities to meet the EV charging demand in this study, and the charging network operator in a demand zone can coordinate and assign the EVs to specific charging facilities. The EVs are then lumped together to form one queue, although the service capacity is split in different locations. Accordingly, a queuing model with unlimited charging facilities $(M/M/\infty)$ is used. The expected queue size of EVs L_q is 0, which yields

$$L = L_s \tag{18}$$

$$L = r = \frac{\lambda}{\mu} \tag{19}$$

where L_s and μ are obtained from the MPC learning model simulations. The stakeholders want to maximize the accessibility of chargers to customers, and at the same time, minimize the investment costs. Therefore, there will not be an infinite number of chargers in practice. The number of charging facilities should be found such that it adequately balances the charging facility needs and the cost of service. $M/M/c$ queuing model with very small queuing delay [35] is used to approximate the $M/M/\infty$ model. The number of charging facilities c in the $M/M/c$ with the probability of queuing α is given by

$$\alpha = \frac{\phi(\beta)}{\phi(\beta) + \beta\Phi(\beta)} \tag{20}$$

$$c \approx r + \beta\sqrt{r} \tag{21}$$

where α is set to 0.01, i.e., the probability that a customer is delayed in the queue during peak hours is 1%. Additionally, $\phi(\cdot)$ and $\Phi(\cdot)$ are the probability density function (PDF) and cumulative distribution function (CDF) of a standard normal random variable.

C. CAPACITY PROVISIONING OF BSSs

The BS time of EVs at BSSs is fixed. Therefore, the $M/D/\infty$ model is used for BSSs. The state probability of $M/D/\infty$ is the same as that of the $M/M/\infty$ model, because the $M/M/\infty$ model is insensitive to the distribution of service time. Hence, λ can be calculated by

$$L = L_s \tag{22}$$

$$L = r = \lambda D \tag{23}$$

where L_s for BSSs is also acquired from the simulation results. Because the delay probability for the $M/M/c$ queue provides a very good approximation to that of the $M/D/c$

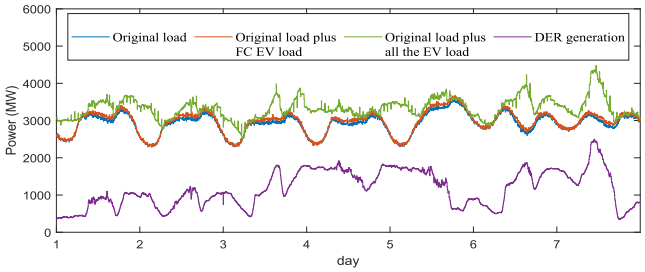

FIGURE 4. EV load impact on the original load profile in the system: base case scenario.

queue [36], equations (20)–(21) can be also used to determine the BS lots for the BSSs.

IV. CASE STUDIES AND NUMERICAL RESULTS

A modified IEEE 118-bus test system in [25] is utilized for the simulations. The test system's original specifications are modified as follows: 3800 MW renewable sources are integrated to the system including one wind farm at bus 24 with the total capacity of 1000 MW and another wind farm with 1500 MV capacity located at bus 27. A 1300 MW photovoltaic (PV) power plant is also added at bus 33. Both weekly predicted and actual data for renewables and load captured in the week of December 18, 2017 in Texas from ERCOT is used in the simulations [37]. Wind power plants, solar farm, and the load have scale factors of 1/8, 1.08, and 1/12.8, respectively. The peak load in the test system is 3,591 MW. The current-day forecast data will replace the day-ahead forecast data in an hour-ahead manner. The curtailment cost of renewables is 40 $/MWh.

The system is assumed to host 900,000 EVs accounting for 90% of all the vehicles. Hence, there is one vehicle per 3.59 kW peak load, which is similar to the real-world vehicle to yearly peak load ratio in the state of Texas in 2017. Note that the vehicle to peak load ratio varies in different regions. The charging and discharging efficiency is assumed 90%. c_d is 12 $/MWh, and the usable EV battery capacity is set to 70 kWh. There are 112,500 EVs only using FC and SFC, 50 kW chargers are used in FC only, 250 kW chargers are used in SFC only, and the inelastic load of the aggregated FC and SFC demand is placed at bus 112. It is assumed that 112,500 EVs only use BS service. The aggregated BSS which is regarded as a virtual battery capacity with 1,050 MWh is placed at bus 117. The BSS charge/discharge rate is set to 242 MW. We add a penalty when the BSS SOC is less than 20%, so 20% of the BSS capacity is reserved for BS. The SOC of the BSS is restricted to be equal or higher than 5%.

The remaining 675,000 EVs use SC methods with the charging rate of 10 kW, and the aggregated SC load is located at bus 115 as a virtual battery. These customers use FC, SFC, or BS as complementary charging methods when their charging demands could not be satisfied by SC alone. Hence, EV customers will swap their depleted battery in BSS when they subscribe to the BS service and the SC mode fails to meet their next trip demand. Otherwise, FC or SFC methods are used based on their charging demand as shown in Fig. 1. The National Household Travel Survey (NHTS) 2017 database [38] is used to obtain the EV driving profiles. We randomly select 10,000 EV driving profiles in the state of Texas to account for the EV customer activities during the simulations. 50% of the EVs are randomly selected to subscribe the BS services. The initial SOC of the EVs has a uniform distribution within 0 to 100% of the battery capacity. 100 to 200 EVs are connected and managed by each aggregator. The estimated upper charging constraint in the first iteration of the MPC learning is based on the availability of the aggregated EVs, and the initial lower charging constraint is set to 0. Aggregated hourly charging constraints from these customers obtained from the simulations are used as the estimated charging constraints during the next iteration. The aggregated EV load is used to estimate the total charging demand. None of these customers is assumed to utilize BS services in the first iteration of the MPC learning, and the actual BS load for these customers obtained from the simulations is used as estimated additive BS energy consumption during the next iteration.

A. SIMULATION RESULTS

We employed the CVX optimizer in MATLAB 2020b to run all the scenarios. 7-day economic dispatch was simulated in the test system utilizing the MPC learning model. The system total operation cost is found $ 9,113,360 after 3 iterations, which is close to the lower bound of the minimum cost ($ 9,065,841). Renewables count for 35.30% of the total generation in the base case scenario. The fuel cost of the conventional generating units is found 25.19 $/MWh on average. Figure 4 illustrates that the FC load for EVs that only use FC and SFC will increase the peak of the original load slightly, as it only counts for a small share of the total power demand of aggregated EVs. The total EV load features a renewable follower characteristic.

Figure 5 shows the number of EVs that are being served in different types of charging stations based on 10,000 sampled EVs in the simulation. Compared with the base case scenario where the EV subscribers for BS service that mainly use SC is 50%, all the unmet charging demands are supplied by the BSS when it has 100% BS service subscription as shown in Fig. 5d, and there is no FC or SFC customer as illustrated in Fig. 5b and Fig. 5c. The BS load is also found with a spike on the 6th day in Fig. 5d. This is because there is less smart charging load around the beginning of the 6th day as shown in Fig. 5a and the system can accordingly integrate more DER power output in the daytime of the 6th day. Thus, the 100% BS service subscription case is featured with higher flexibility under given BSS capacity, and the average fuel cost is 25.15 $/MWh, which is lower than that of the base case scenario. However, when it has 0% BS service subscription, there are still some customers using BS service as shown in Fig. 5d. The reason lies in the fact that a few EVs have long driving distance, and their charging demand could not be met by FC or SFC. The fuel cost is 25.22 $/MWh on average

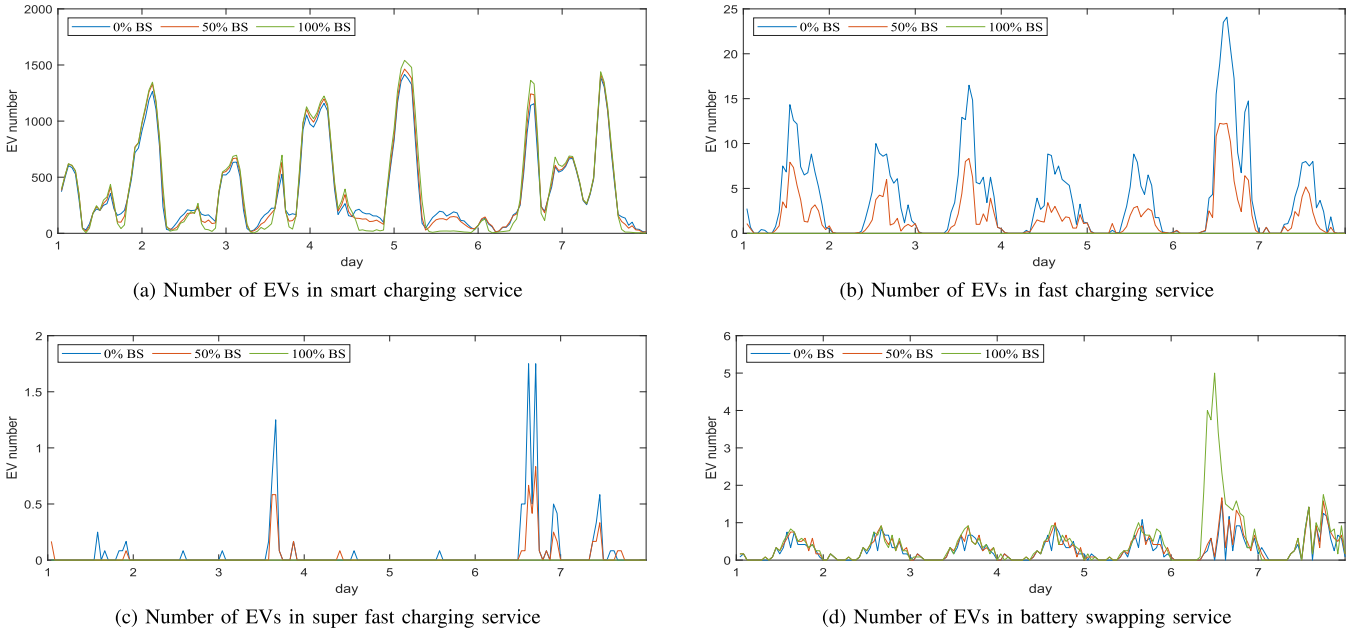

(a) Number of EVs in smart charging service

(b) Number of EVs in fast charging service

(c) Number of EVs in super fast charging service

(d) Number of EVs in battery swapping service

FIGURE 5. Hourly average number of EVs in different types of charging stations with 0%, 50% and 100% subscription of the BS service for the 10,000 smart charging EVs in the sample.

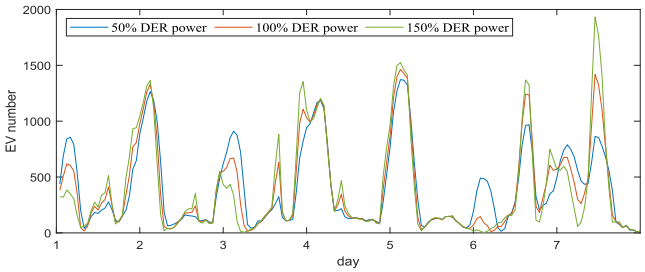

FIGURE 6. Comparison of the hourly average number of EVs with smart charging service under 50%, 100% and 150% DER power generation for 10,000 EVs in the sample.

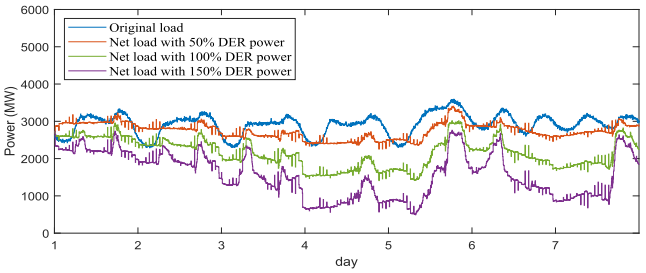

FIGURE 7. Comparison of the original load and the net load profiles under 50%, 100% and 150% DER power generation in the system.

which is higher than that of the base case scenario. This is because more FC load will result in more inelastic load for the system to supply. To our best knowledge, this is the first effort in the literature to indicate how the change of the BS service subscription ratio could affect FC, SFC and SC loads.

B. IMPACTS OF DER AND EV PENETRATION ON THE POWER GRID

Different DER capacities are also simulated to show the impacts of DER integration on EV charging demands. The comparison results of the base case scenario with 100% DER capacity are shown in Fig. 6. With the increase in DER power generation, there are more SC EV loads matching DER power output instead of filling the off-peak load valley. In the scenario with 150% DER power output, the system needs more EV charging loads in the 7th day than the daily peak times in the week to match the high DER power generation. It indicates that the system needs more SC chargers or stationary storage units to avoid DER energy curtailment when DER penetration level is high. FC, SFC and BS curves slightly change, because the number of EVs that need these services are small and stable. As demonstrated in Fig. 7, the DER penetration levels also affect the net load in the system, which is the load demand supplied by conventional generators. Higher DER penetrations result in lower minimum output and higher ramp rate of the conventional generating units. We define the ramp factor as the minimum load divided by the maximum load during a time period. The total energy supplied by DERs in percentage and the ramp factor of the system are shown in Table 1. It can be seen that even with 90% EV penetration to match DER power output, the system still needs higher ramp-rate generators and more storage units to maintain the system stability and improve the ramp factor when the DERs have 150% power output and supply 52.92% of the system load. Therefore, the aggregated EV charging load can also participate in the frequency responses to maintain the system stability.

The simulation results for 60% and 30% EV penetration levels in the system are also added to Table 1. It can be seen that the scenario with 30% EV penetration level and 150%

TABLE 1. System performance Indices under Different DER Integration Scenarios.

DER Power Output (%)		50	100	150
90% EV Penetration	DER ratio (%)	17.64	35.30	52.92
	Ramp factor	0.66	0.47	0.18
60% EV Penetration	DER ratio (%)	18.39	36.79	55.16
	Ramp factor	0.62	0.38	0.08
30% EV Penetration	DER ratio (%)	19.22	38.45	57.68
	Ramp factor	0.56	0.33	0.03

TABLE 2. Capacity Provisioning Results In The Base Case Scenario.

Charging method	SC	FC	SFC	BS
L_s	1464	12.25	0.83	1.67
T (min)	-	9.45	6.3	5
T' (min)	-	15	10	5
c	2091	30	4	5
L_q	-	0.03	0.03	0.01

DER power output is found with a very low ramp factor, when the DERs supply 57.68% of the system total load. Accordingly, if the system planner considers to increase the DER penetration level first, followed by an increase in EV penetration, then the power grid stability status will be a great concern. On the other hand, the system will have high ramp factor with 90% EV penetration level and 50% DER power output. However, when the system planner firstly increases EV penetration and then considers to adopt more DERs, the low ratio of DER energy supply to the total energy supply may affect the reduction of carbon emissions in the early stages. Hence, the coordinated expansion of the EVCI and DERs are needed to trade off less impact to grid stability and more DER energy supply for clean energy transition.

C. CAPACITY OF DIFFERENT CHARGING STATIONS

Table 2 shows the results on the number of different EV chargers and battery swapping lots for 10,000 sampled EVs in the base case scenario with 90% EV penetration and 100% DER power output. L_s is the maximum number of EVs that are in the service for each charging method, and is obtained from Fig. 5. 30% of the SC capacity is reserved considering the uncertainty of the EV customer behaviors and those inherent to the system. The queuing models are used for FC, SFC and BSS services. The average service times T for FC and SFC are also obtained from simulations. We extend both to 15 minutes and 10 minutes respectively, considering the idle parking time, and name it as T'. The average service time for BSS is assumed to be 5 minutes. With calculated charging capacity c for the 10,000 EVs using equations (20)-(21), the average number of EVs in the queue L_q during the peak hours is very small, which highlights that the designed charging capacities are promising approximation of the ideal charging stations without queuing, and few customers will experience delay (similar to the case of gas stations).

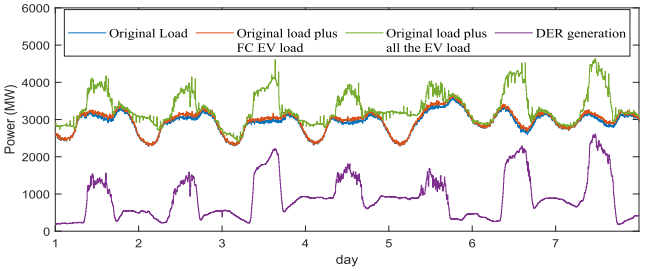

FIGURE 8. EV load impact on the original load profile in the system: California scenario.

Based on the results presented in Table 2, if the SC chargers can be installed all over the charging demand zone, a residential parking garage with 200 EVs should have 42 or more 10 kW chargers. The total number of charging facilities needed for FCS, SFCS and BSS in the zone are small, so the charging facilities should be placed near the high traffic flow areas or highways.

D. SENSITIVITY ANALYSIS

1) IMPACTS OF DIFFERENT EV CUSTOMER BEHAVIORS AND REGIONS

The driving profiles of 10,000 customers in the state of California are randomly selected to simulate the impact of EV customer behaviors to the EVCI expansion planning in different regions. Also, compared to the studied base case, the total capacity of wind and solar farms are reversed so that wind power plant is 1,300 MW and PV power plant is 2,500 MW. Figure 8 illustrates that the aggregated SC EVs still show the renewable follower characteristic. But compared to Fig. 4, there are more charging sessions during the daytime since solar power generation is higher in this scenario. The capacity provisioning results for 10,000 sampled EVs in the California scenario are also demonstrated in Table 3. Compared to Table 2 in the base case under the same 50% BS subscription ratio, it indicates that more SC facilities are needed to match the higher solar power during the daytime. The number of FC and SFC facilities increases since more SC sessions are scheduled during the daytime and the customers sometimes need more FC or SFC service in order to handle the daily trip demand. However, the demand for BS swapping lots is reduced. This is because the daily average driving distance for these sampled EVs in California is less than that of customers in Texas, where higher customer trip energy demands could be met by only using SC even though they subscribe the BS service. Less demand of complementary BS service also contributes to the increased usage of the SC facilities. Note that we rounded up the charging capacity c to the smaller integer greater than or equal to the calculated values, so the L_q results in Table 2 and Table 3 are slightly different.

2) COMPUTATION PERFORMANCE

All the simulations are done on a 3.10GHz Intel i5 Core 16 GB RAM computer. The total execution time of the base case scenario with 10,000 EV samples is 183 minutes.

TABLE 3. Capacity Provisioning Results in The California Scenario.

Charging method	SC	FC	SFC	BS
L_s	1587	13.3	1.4	1.0
T (min)	-	10.65	6.9	5
T' (min)	-	16.2	10.6	5
c	2267	31	6	3
L_q	-	0.03	0.01	0.02

TABLE 4. Computation Results of MPC Learning Under Different EV Samples.

Samples	unit cost ($/MWh)	average time (min)	iteration
2,000	25.20	43.4	4
10,000	25.19	45.8	4
50,000	25.17	52.7	4

The average time for each iteration is 45.8 minutes, and the simulation is terminated after 4 iterations as shown in Table 4. 7 days simulation is run during each iteration, and the calculation time includes the 24-hour look-ahead direct current optimal power flow (DCOPF) execution in the outer MPC loop with a time step of 1 hour, the 3-hour look-ahead DCOPF execution in the inner MPC loop with a time step of 5 minutes, and the computation time of aggregating individual EV charging constraints and calculating power allocated to EVs which are happening every 5 minutes. As illustrated in Table 4, the average computation time during each iteration only increases by 7 minutes when we increase the EV samples from 10,000 to 50,000. The simulation time in each iteration does not increase significantly since aggregation of individual EV parameters and power allocation to each EV are arithmetical calculations, and the DCOPF model is a convex optimization using the aggregated information. Also, the computation of the EVCI planning problem can be done offline. Hence, the model can be scaled to large EV data samples. However, the limited customer travel data will be a main concern when simulating larger EV samples in a region, as we imported NHTS customer data from 12 states including Texas, California, Washington, etc., to reach 50,000 EV samples in the simulation. Also, customer behavior in different regions may vary which affects the average unit cost of generators in the simulation.

3) EFFECT OF APPLYING THE PROPOSED MODEL TO MEDIUM VOLTAGE (MV) AND LOW VOLTAGE (LV) SYSTEMS

The higher-level look-ahead economic dispatch model solves multiple future time-step dispatch problems during each time step. The power flow is a DCOPF formulation and power losses are not considered. The load values in our look-ahead economic dispatch model can be increased to account for the estimated losses, and the mathematical formulation remains the same. The voltage drops are also not included in the look-ahead DCOPF model. AC feasibility check following DCOPF solutions can ensure that the solutions are applicable in real-world operation of the high voltage transmission system. The voltage drops in distribution system are implicitly accounted for by the proposed method since the SC could avoid the increase in peak loads. The voltage drops and reactive power in the distribution grid can be also compensated locally by EV charging stations and regulating transformers, if the EV charging stations can operate in four-quadrants. Since this paper aims at regional-level EVCI expansion planning, the distribution voltage drops are not considered in the model in order to balance the modeling precision and computational complexity in this planning problem. However, the proposed model can be used to simulate the MV or LV system when ACOPF is used to consider distribution system voltage drops and power losses, as the proposed model itself can simulate different EV sample sizes. One needs to only take into account that the total EV and simulated EV are required to have a relatively large number so that the aggregated EV parameters are predictable and the cost production model can be used. Also, the number of customers using FC, SFC and BS will be much smaller than that of using SC. The FCS, SFCS and BSS planning results will be more accurate with large number of EV samples.

V. DISCUSSIONS

The simulation results provide an estimation of the charging load ratio in a region when SC can be installed in most locations. The results show that the number of customers using FC, SFC or BSS will be much smaller than that of using SC, and SC of large-scale EVs could optimize the system cost and improve the system performance by increasing its flexibility. While BS service is necessary considering the long-drive distances of a few EVs, the stakeholders can still use FC and SFC to replace BSS as long as EV customers are willing to spend some time to charge their EVs during the trip. Also, the FC and SFC are good companions for customers who do not subscribe a BS service. In the studied case in California with the same BS subscription ratio as that in the base case, the FC and SFC capacity increase. The large solar power will supply the increased FC and SFC load and mitigate the impacts of FC and SFC to the power grid. In contrast, BSSs are less needed. Hence, the actual ratio of the BSSs will be determined by customer preference and the grid flexibility needs.

The interaction of the future large-scale EV loads and DERs is also studied. The obtained performance indices of the power grid can guide the regional expansion planning with massive deployment of EVCI and DERs. System planners and electric utility regulators can determine the trajectory of the EVCI and DER expansion based on Table 1. The planning results can also be adjusted based on the system parameter changes over time.

The charging capacity in a local charging demand zone is also calculated, which returns an upper bound for the minimum charging facilities in most cases. However, the placement of specific charging stations in an area should be studied case by case. For example, each household should have one level-2 SC charger if they can install it. Coverage is

also an important factor for selecting the locations of FCSs, SFCSs, and BSSs as they may be in less demand. More FC facilities should be built to cover the whole area even if some of them have a low utilization rate. Other factors such as land use, customer density, traffic density, power distribution grid and customer preferences should also be considered. If most EV customers in the area cannot install the charging at home or workplace, the FC, SFC or BS stations will be the main charging method; the planning is then similar to that of a gas station. Once the arrival rate and charging time of the charging stations are estimated, the queuing models in this paper can still be used to decide on the number of charging facilities. If the area has mixed SC customers, and BS or FC only customers, it requires the stakeholders to observe the portion of different types of customers, follow the cite guidelines and plan accordingly with a combination of different methods. The detailed location and placement methods of DERs and EV charging facilities [39] are out of scope of this paper.

The simulated charging capacity of different charging facilities can be used as a starting point for detailed EVCI planning. With the estimated future charging capacities in a charging demand zone, experts in different domains can then study land use, potential locations, and configurations of different types of the charging stations. It enables the backward planning of the EVCIs since the coordinated planning considers different EV and renewable penetration levels, and avoids a situation where the charging stations are built based on current charging demand and will need costly facility upgrades later. During the forward expansion processes, a certain number of EV supply equipment and DERs can be added based on the diffusion speed of EVs and a certain level of charging facility adequacy should be maintained.

VI. CONCLUSION

This article discussed three aspects of EVCI expansion planning considering the increasing trend in DER penetration. Firstly, the proposed method can quantify the change in the EV charging load ratio with respect to the changes in EV charging methods. Hence, the equilibrium of EV charging load ratio in future smart grids can be simulated. Besides, different EV and DER penetration levels are also simulated. The appropriate penetration levels can be set by system planners and electric utility regulators to trade off the DER energy supply expectation and the power grid stability concerns. Furthermore, the charging capacities of different charging stations are also quantified to achieve the equilibrium of adequate charging facilities for customers and less investment cost for stakeholders. The results of these considerations help to optimize the strategic planning to achieve a smooth clean energy transition. While these trade off decisions can vary in different geographical regions, and change dynamically when system parameters evolve over time, the decision makers can still simulate the results using the proposed methods with new parameter values, and change the action policy with updated planning targets. They can also adjust the planning target based on the expansion outcomes in practice.

Several important aspects that could be further researched in the future include (i) building co-optimization model for transmission and distribution systems to more accurately model power losses and voltage drops; (ii) considering capabilities and locations of DERs and EV charging stations to better plan and operate the power distribution grids.

REFERENCES

[1] IEA. (2021). *Net Zero by 2050*. Accessed: Jan. 7, 2023. [Online]. Available: https://www.iea.org/reports/net-zero-by-2050

[2] N. Mehboob, M. Restrepo, C. A. Cañizares, C. Rosenberg, and M. Kazerani, "Smart operation of electric vehicles with four-quadrant chargers considering uncertainties," *IEEE Trans. Smart Grid*, vol. 10, no. 3, pp. 2999–3009, May 2019.

[3] B. Wang, P. Dehghanian, S. Wang, and M. Mitolo, "Electrical safety considerations in large-scale electric vehicle charging stations," *IEEE Trans. Ind. Appl.*, vol. 55, no. 6, pp. 6603–6612, Nov. 2019.

[4] B. Wang, J. A. Camacho, G. M. Pulliam, A. H. Etemadi, and P. Dehghanian, "New reward and penalty scheme for electric distribution utilities employing load-based reliability indices," *IET Gener., Transmiss. Distrib.*, vol. 12, no. 15, pp. 3647–3654, Aug. 2018.

[5] S. Rajakaruna, F. Shahnia, and A. Ghosh, *Plug in Electric Vehicles in Smart Grids: Integration Techniques* (Power Systems). Singapore: Springer, 2014.

[6] M. Straka et al., "Predicting popularity of electric vehicle charging infrastructure in urban context," *IEEE Access*, vol. 8, pp. 11315–11327, 2020.

[7] S. Bae and A. Kwasinski, "Spatial and temporal model of electric vehicle charging demand," *IEEE Trans. Smart Grid*, vol. 3, no. 1, pp. 394–403, Mar. 2012.

[8] W. Infante and J. Ma, "Coordinated management and ratio assessment of electric vehicle charging facilities," *IEEE Trans. Ind. Appl.*, vol. 56, no. 5, pp. 5955–5962, Sep. 2020.

[9] A. Moradipari and M. Alizadeh, "Pricing and routing mechanisms for differentiated services in an electric vehicle public charging station network," *IEEE Trans. Smart Grid*, vol. 11, no. 2, pp. 1489–1499, Mar. 2020.

[10] H. Zhang, Z. Hu, and Y. Song, "Power and transport nexus: Routing electric vehicles to promote renewable power integration," *IEEE Trans. Smart Grid*, vol. 11, no. 4, pp. 3291–3301, Jul. 2020.

[11] H. Parastvand, V. Moghaddam, O. Bass, M. A. S. Masoum, A. Chapman, and S. Lachowicz, "A graph automorphic approach for placement and sizing of charging stations in EV network considering traffic," *IEEE Trans. Smart Grid*, vol. 11, no. 5, pp. 4190–4200, Sep. 2020.

[12] W. Gan et al., "Coordinated planning of transportation and electric power networks with the proliferation of electric vehicles," *IEEE Trans. Smart Grid*, vol. 11, no. 5, pp. 4005–4016, Sep. 2020.

[13] F. Xie and Z. Lin, "Integrated U.S. nationwide corridor charging infrastructure planning for mass electrification of inter-city trips," *Appl. Energy*, vol. 298, Sep. 2021, Art. no. 117142.

[14] F. Elghitani and E. F. El-Saadany, "Efficient assignment of electric vehicles to charging stations," *IEEE Trans. Smart Grid*, vol. 12, no. 1, pp. 761–773, Jan. 2021.

[15] B. Badia, R. A. Berry, and E. Wei, "Investment in EV charging spots for parking," *IEEE Trans. Netw. Sci. Eng.*, vol. 7, no. 2, pp. 650–661, Apr. 2020.

[16] C. J. R. Sheppard, A. Harris, and A. R. Gopal, "Cost-effective siting of electric vehicle charging infrastructure with agent-based modeling," *IEEE Trans. Transport. Electrific.*, vol. 2, no. 2, pp. 174–189, Jun. 2016.

[17] R. Rudnik, C. Wang, L. Reyes-Chamorro, J. Achara, J.-Y.-L. Boudec, and M. Paolone, "Real-time control of an electric vehicle charging station while tracking an aggregated power setpoint," *IEEE Trans. Ind. Appl.*, vol. 56, no. 5, pp. 5750–5761, Sep. 2020.

[18] K. Sepetanc and H. Pandzic, "A cluster-based operation model of aggregated battery swapping stations," *IEEE Trans. Power Syst.*, vol. 35, no. 1, pp. 249–260, Jan. 2020.

[19] International Renewable Energy Agency. *Global Energy Transformation: A Roadmap to 2050 (2019 Edition)*. Accessed: Jan. 7, 2023. [Online]. Available: https://www.irena.org/publications/2019/Apr/Global-energy-transformation-A-roadmap-to-2050-2019Edition

[20] T. Unterluggauer, J. Rich, P. B. Andersen, and S. Hashemi, "Electric vehicle charging infrastructure planning for integrated transportation and power distribution networks: A review," *eTransportation*, vol. 12, May 2022, Art. no. 100163. [Online]. Available: https://www.sciencedirect.com/science/article/pii/S2590116822000091
[21] C. Li, Z. Dong, G. Chen, B. Zhou, J. Zhang, and X. Yu, "Data-driven planning of electric vehicle charging infrastructure: A case study of Sydney, Australia," *IEEE Trans. Smart Grid*, vol. 12, no. 4, pp. 3289–3304, Jul. 2021.
[22] C. Lei, L. Lu, and Y. Ouyang, "System of systems model for planning electric vehicle charging infrastructure in intercity transportation networks under emission consideration," *IEEE Trans. Intell. Transp. Syst.*, vol. 23, no. 7, pp. 8103–8113, Jul. 2022.
[23] A. Almutairi and O. Alrumayh, "Optimal charging infrastructure portfolio for minimizing grid impact of plug-in electric vehicles," *IEEE Trans. Ind. Informat.*, vol. 18, no. 8, pp. 5712–5721, Aug. 2022.
[24] B. Wang, P. Dehghanian, and D. Zhao, "Chance-constrained energy management system for power grids with high proliferation of renewables and electric vehicles," *IEEE Trans. Smart Grid*, vol. 11, no. 3, pp. 2324–2336, May 2020.
[25] B. Wang, D. Zhao, P. Dehghanian, Y. Tian, and T. Hong, "Aggregated electric vehicle load modeling in large-scale electric power systems," *IEEE Trans. Ind. Appl.*, vol. 56, no. 5, pp. 5796–5810, Sep. 2020.
[26] R. Wolbertus and R. Van den Hoed, "Electric vehicle fast charging needs in cities and along corridors," *World Electr. Vehicle J.*, vol. 10, no. 2, p. 45, Jun. 2019. [Online]. Available: https://www.mdpi.com/2032-6653/10/2/45
[27] V. Cherkassky, *Predictive Learning*. Minneapolis, MN, USA: VCtextbook, 2013, ch. 1.
[28] S. Chatzivasileiadis, A. Venzke, J. Stiasny, and G. Misyris, "Machine learning in power systems: Is it time to trust it?" *IEEE Power Energy Mag.*, vol. 20, no. 3, pp. 32–41, May 2022.
[29] S. Bhattacharyya, D. Cofer, D. Musliner, J. Mueller, and E. Engstrom, "Certification considerations for adaptive systems," in *Proc. Int. Conf. Unmanned Aircr. Syst. (ICUAS)*, Jun. 2015, pp. 270–279.
[30] I. D. Landau, R. Lozano, M. M'Saad, and A. Karimi, *Adaptive Control* (Communications and Control Engineering). London, U.K.: Springer, 2011.
[31] Y. Tao, J. Qiu, S. Lai, X. Sun, and J. Zhao, "A data-driven agent-based planning strategy of fast-charging stations for electric vehicles," *IEEE Trans. Sustain. Energy*, early access, Dec. 28, 2022, doi: 10.1109/TSTE.2022.3232594.
[32] W. Tan, Y. Sun, Z. Ding, and W.-J. Lee, "Fleet management and charging scheduling for shared mobility-on-demand system: A systematic review," *IEEE Open Access J. Power Energy*, vol. 9, pp. 425–436, 2022.
[33] O. Ahmed, L. Hocine, H. Lamia, and M. Meriem, "Maximum power point tracking in photovoltaic system using indirect adaptative control," in *Proc. 1st Int. Conf. Sustain. Renew. Energy Syst. Appl. (ICSRESA)*, Dec. 2019, pp. 1–6.
[34] R. Pagany, L. R. Camargo, and W. Dorner, "A review of spatial localization methodologies for the electric vehicle charging infrastructure," *Int. J. Sustain. Transp.*, vol. 13, no. 6, pp. 433–449, 2019.
[35] D. Gross, J. Shortle, J. Thompson, and C. Harris, *Fundamentals of Queueing Theory* (Wiley Series in Probability and Statistics). Hoboken, NJ, USA: Wiley, 2011.
[36] H. C. Tijms, "New and old results for the M/D/c queue," *AEU Int. J. Electron. Commun.*, vol. 60, no. 2, pp. 125–130, Feb. 2006.
[37] *ERCOT*. Accessed: Jan. 7, 2023. [Online]. Available: http://www.ercot.com/gridinfo
[38] U.S. Department of Transportation. *2017 National Household Travel Survey*. Accessed: Jan. 7, 2023. [Online]. Available: https://nhts.ornl.gov
[39] I. S. Bayram and S. Bayhan, "Location analysis of electric vehicle charging stations for maximum capacity and coverage," in *Proc. IEEE 14th Int. Conf. Compat., Power Electron. Power Eng. (CPE-POWERENG)*, Jul. 2020, pp. 409–414.

BO WANG (Member, IEEE) received the B.Sc. degree in automation from Jilin University, Changchun, China, in 2013, the M.Sc. and Ph.D. degrees in electrical engineering from George Washington University, Washington, DC, USA, in 2015 and 2020, respectively.

He is currently a Power Electronics Engineer with Amazon Web Services, Seattle, Washington. His research interests include electric vehicles, power system optimization and control, and smart grid reliability.

PAYMAN DEHGHANIAN (Senior Member, IEEE) received the B.Sc. degree in electrical engineering from the University of Tehran, Tehran, Iran, in 2009, the M.Sc. degree in electrical engineering from the Sharif University of Technology, Tehran, in 2011, and the Ph.D. degree in electrical engineering from Texas A&M University, TX, USA, in 2017. He is currently an Assistant Professor with the Department of Electrical and Computer Engineering, George Washington University, Washington, DC, USA. His research interests include power system reliability and resilience assessment, data-informed decision-making for maintenance and asset management in electrical systems, and smart electricity grid applications.

He was a recipient of the 2014 and 2015 IEEE Region 5 Outstanding Professional Achievement Award, the 2015 IEEE-HKN Outstanding Young Professional Award, the 2021 Early Career Award from the Washington Academy of Sciences, and the 2022 Early Career Researcher Award from George Washington University.

DONGBO ZHAO (Senior Member, IEEE) received the B.S. degree from Tsinghua University, Beijing, China, the M.S. degree from Texas A&M University, College Station, TX, USA, and the Ph.D. degree from the Georgia Institute of Technology, Atlanta, Georgia, all in electrical engineering.

He is currently a Global Technology Manager with the Eaton Research Laboratory, Eaton. He was a Team Leader of DER integration and a Principal Energy System Scientist with the Argonne National Laboratory, Lemont, IL, USA, and an Institute fellow of the Northwestern Argonne Institute of Science and Engineering, Northwestern University, before joining Eaton. His research interests include power system control, protection, reliability analysis, transmission and distribution automation, and electric market optimization.

Dr. Zhao is a member of IEEE PES, IAS, and IES Societies. He was an Editor of IEEE TRANSACTIONS ON POWER DELIVERY, IEEE TRANSACTIONS ON SUSTAINABLE ENERGY, and IEEE POWER ENGINEERING LETTERS.